Cell Reports
Physical Science

Article

Intelligent wearable system design for personalized knee motion and swelling monitoring in osteoarthritis care

Graphical abstract

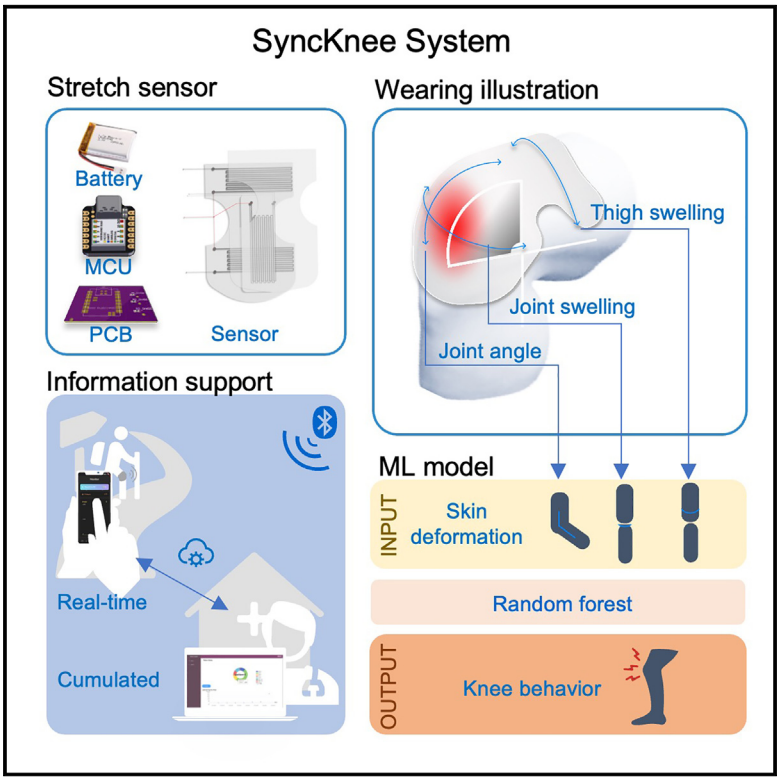

Highlights

- A wearable system for measuring the human knee state with motion and swelling patterns
- A strain sensor constructed from poly(SBS) fiber and EGaIn alloy
- Utilizing the random forest algorithm to classify knee behavior precisely
- A personal information system that supports both real-time and accumulated analysis

Authors

Zhengtao Ma, Le Fang, Cong Fang, ..., Bo Chai, Zijian Zheng, Stephen Jia Wang

Correspondence

stephen.j.wang@polyu.edu.hk

In brief

This study presents a soft, wearable system that leverages stretchable sensors and machine learning to measure knee-joint angles and swelling patterns, offering real-time monitoring and cumulative insights for managing osteoarthritis.

Ma et al., 2025, Cell Reports Physical Science 6, 102438
March 19, 2025
https://doi.org/10.1016/j.xcrp.2025.102438

CellPress

Cell Reports
Physical Science

CellPress
OPEN ACCESS

Article

Intelligent wearable system design for personalized knee motion and swelling monitoring in osteoarthritis care

Zhengtao Ma,[1,2] Le Fang,[1] Cong Fang,[1] Fan Chen,[3] Sark Pangrui Xing,[1] Bo Chai,[1] Zijian Zheng,[3] and Stephen Jia Wang[1,2,4,*]

[1]School of Design, The Hong Kong Polytechnic University, Hong Kong SAR, China
[2]Laboratory of Artificial Intelligence in Design, Hong Kong SAR, China
[3]Laboratory for Advanced Interfacial Materials and Devices, School of Fashion and Textiles, The Hong Kong Polytechnic University, Hong Kong SAR, China
[4]Lead contact
*Correspondence: stephen.j.wang@polyu.edu.hk
https://doi.org/10.1016/j.xcrp.2025.102438

SUMMARY

Daily knee monitoring is critical for osteoarthritis management, aiding in both prevention and rehabilitation. Current wearable solutions for daily use typically capture knee-bending angles as a single feature but lack evidence for comprehensive knee-state recognition. Here we introduce SyncKnee, a knee-monitoring system that tracks both joint angles and swelling patterns, providing detailed knee-state monitoring for daily use. SyncKnee consists of three components: a stretch sensor pad, a multi-modal machine-learning model, and personalized information support. The sensor, made from poly(SBS) fiber and eutectic gallium-indium alloy, tracks skin deformation from bending and swelling. Robotic-arm-driven tests confirm sensor accuracy in responding to bending and swelling. In the user study with 15 participants performing five distinct knee maneuvers, our system with a random forest model achieves 98.48% accuracy in recognizing knee behaviors. SyncKnee offers a comprehensive approach to knee monitoring with promising applications for daily osteoarthritis care.

INTRODUCTION

Knee osteoarthritis (KOA) is a prevalent condition. In 2019, the World Health Organization estimated that approximately 528 million people worldwide were affected by osteoarthritis (OA), with the knee being one of the most commonly involved joints.[1] KOA severely impairs mobility and quality of life while increasing the risk of falls and fractures.[2,3] Consequently, the importance of daily knee monitoring has grown, providing valuable insights into personalized knee-movement tracking[4,5] and supporting the prediction and assessment of KOA progression and rehabilitation outcomes.[6]

Fixed knee-monitoring technologies used in hospitals and laboratories, such as magnetic resonance imaging (MRI)[7] and vision-based motion-capture systems,[8] are costly and space demanding, making them impractical for individuals to use for daily knee-health tracking at home. In contrast, wearable knee-monitoring devices enable convenient daily tracking.

Wearable knee-monitoring devices are critically evaluated for their ability to provide comprehensive data, achieve accurate motion recognition, and offer adequate comfort. Previous studies have employed inertial measurement units (IMUs)[9,10] or physiological sensors, such as galvanic skin response sensors,[11] to function as goniometers, providing data on knee angles and motion frequency.[3] However, single-angle data have limited clinical acceptance, emphasizing the need for multi-channel data on knee characteristics, such as muscle and joint swelling.[12] In previous clinical research, swelling acts as one characteristic of knee abnormality[13] and indicates knee problems such as KOA or an overused knee state after workout.[3,12] Nowadays, swelling measurement is usually limited in clinics with experienced physiotherapists. The swelling measurement on outpatients commonly uses surface circumference measurements to indicate the quantification of leg edema.[14,15] To address the gap of missing wearable swelling measurements, our study aims to incorporate knee-surface displacement and customize a wearable sensor capable of estimating both knee-flexion angle and swelling.

Additionally, considering behavior recognition, machine-learning (ML) techniques have shown high accuracy in recognizing complex or subtle motion patterns,[11,16,17] suggesting that multi-channel data inputs could enhance the detection of intricate knee-movement patterns.

From a comfort standpoint, the dynamic shape of the knee makes rigid sensors such as IMUs uncomfortable for extended wear. Advances in materials science have led to the development of soft strain gauges made from fiber substrates and liquid conductors, providing greater comfort when worn on the skin.[18,19] However, the studies on soft strain gauges primarily focus on

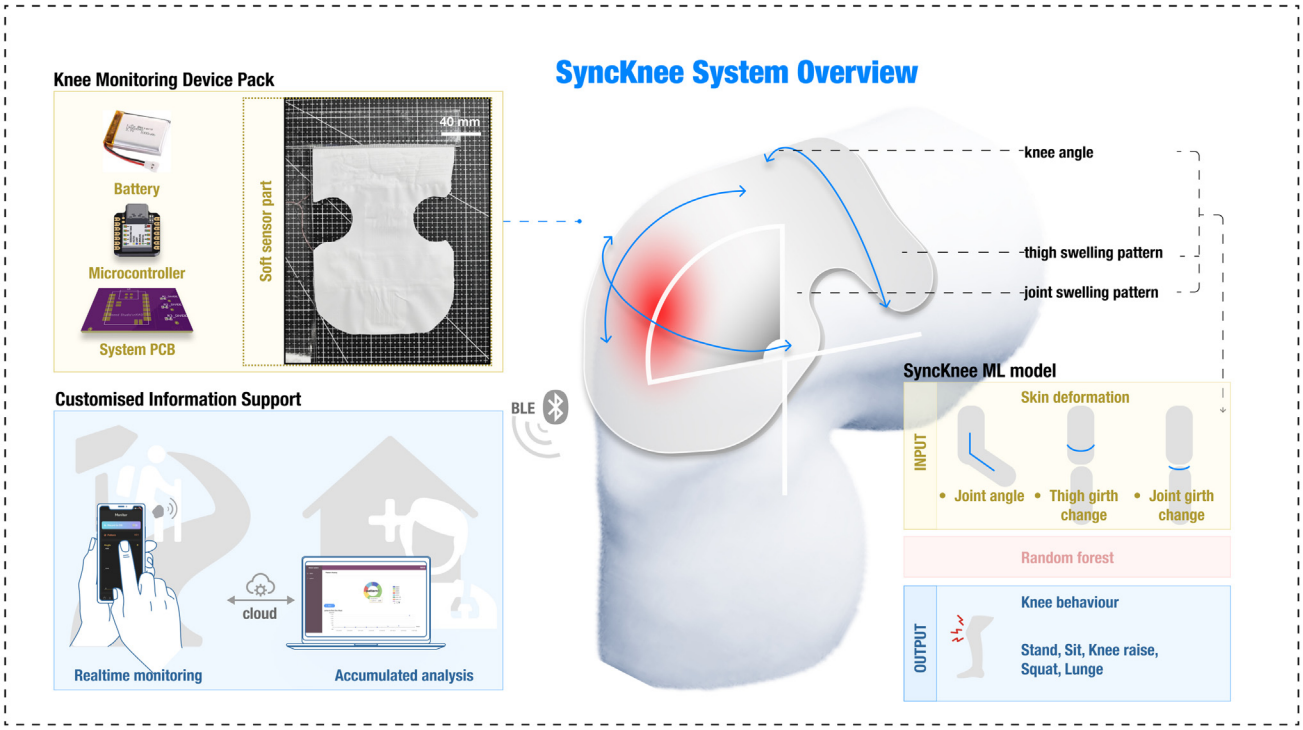

Figure 1. Overview of the SyncKnee system

The SyncKnee system includes a knee-monitoring device, an information support system, and a multi-modal model for assessing knee conditions.

hardware implementation, lacking a unified approach that integrates ML-enhanced monitoring and user-friendly personal data display. This gap complicates the ability of patients with KOA, or individuals tracking daily knee exercises, to interpret and utilize the collected data effectively.

In summary, current wearable knee-monitoring solutions suffer from two main issues related to hardware and software: (1) while swelling and kinematics are crucial for observing knee states, current wearable sensors predominantly assess only kinematic data; and (2) targeting personal usage, present knee monitoring lacks a unified solution that integrates knee-swelling pattern recognition with data display tailored for individual users. Therefore, this paper introduces SyncKnee, an ML-enabled wearable knee-monitoring system accompanied by a personal information display, designed for individual users' OA prevention and rehabilitation. An overview of the SyncKnee system is shown in Figure 1.

This paper presents three main contributions.

(1) Three-dimensional knee monitoring. A stretchable knee-monitoring device is designed for assessing three-dimensional knee skin deformation, capturing the physical factors on users' knees, i.e., joint angle, joint girth, and thigh girth.

(2) A multi-modal model for real-time knee monitoring. The random forest machine model is adopted to recognize the angle and swelling status of the knee based on the data from multiple modalities, including the knee's displacement signals in the direction of joint flexion and the joint circle.

(3) App and website for personal information support. A personal app and website are proposed to show the knee data and help users perceive their knee state through real-time knee monitoring and accumulated knee-status analysis.

In the following sections, we present our comprehensive knee-monitoring system, SyncKnee, detailing sensor characterization and the ML model. Two types of experiments were conducted to assess the system's feasibility: one involving customized in-lab knee-movement simulators for technical evaluation and the other with real users. Rigorous evaluation with 15 participants demonstrates the system's effectiveness, with a random forest model achieving 98.48% accuracy in classifying five distinct knee maneuvers. These results demonstrate the system's technical robustness and practical feasibility. We conclude by synthesizing key takeaways from the study and discussing potential applications of SyncKnee in daily OA care.

RESULTS

SyncKnee hardware design and characterization

Material composition

In this study, a stretch sensor unit characterized by a three-layered architecture (Figure 2A) was specifically devised for the evaluation of skin deformation on the knee. This construct consists of a stretchable material that functions as the insulating substrate layer (adjacent to the human skin), an outer protective

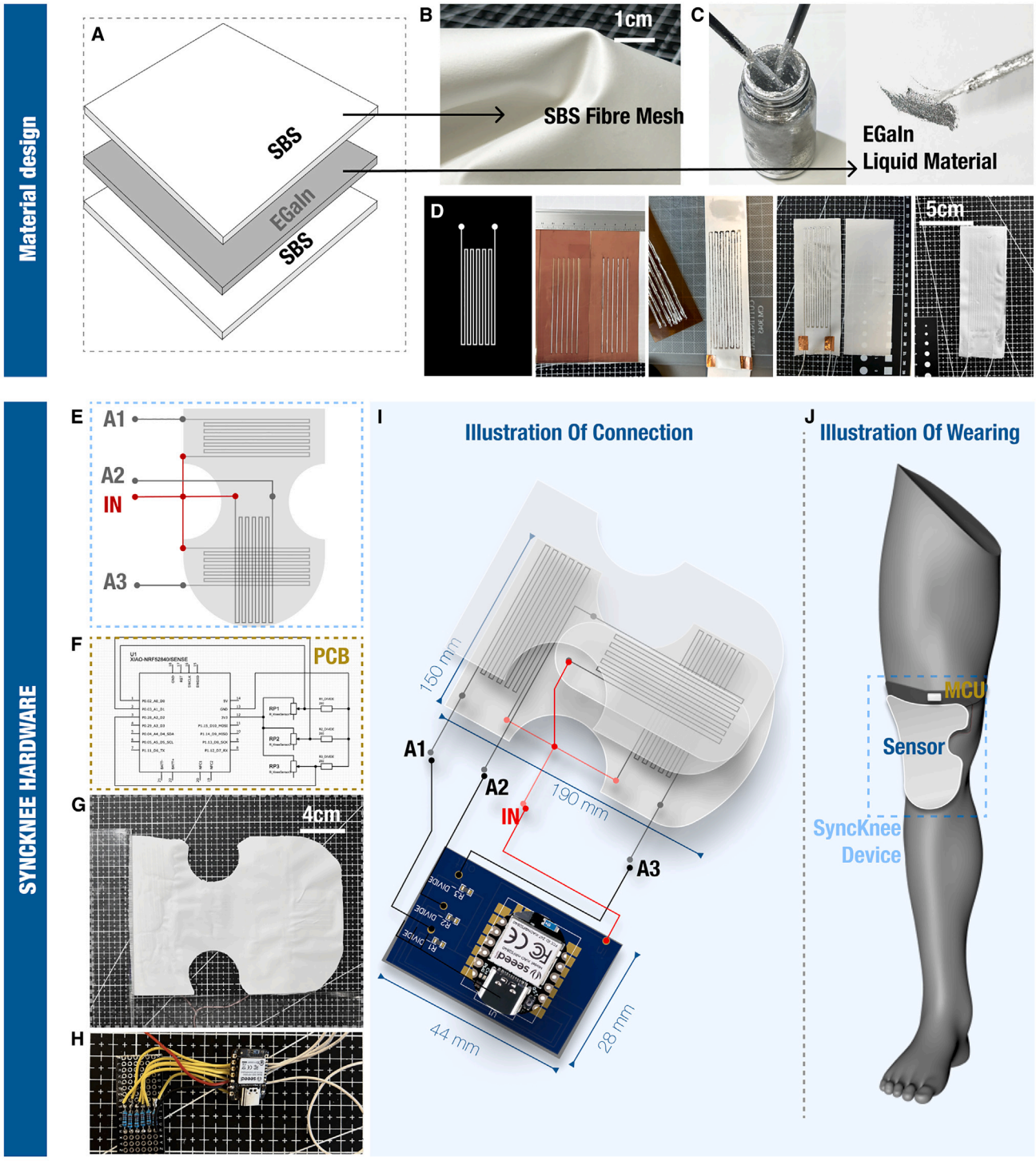

Figure 2. SyncKnee design

(A–D) 1: materials design. (A and B) poly(SBS) fiber-mat substrate and (C) EGaIn liquid metal. (D) Sensor printing process: stencil pattern design, stencil cutting, liquid metal printing, connecting wires, and gluing the top layer.

(E–J) 2: hardware overview. (E and F) Circuit design of the sensor. (G and H) Actual sensor mat size and PCB. (I) Connection of sensing part and PCB. (J) Illustration of wearing location.

Table 1. Comparison of three main flexible electronic substrate materials

Material choice	Reference	Stretchable	Breathable	Thickness (mm)
PI	Wang et al.[21]	no	no	0.24
PDMS	Tokuda et al.[18]	yes	no	≈1
Poly(SBS) fiber mat	Ma et al.[22]	yes	yes	0.2

layer (adjacent to the air), and an intermediary conductive material situated between these two layers. As a human-centered design, the base layer should be stretchable and skin-friendly. The entire three-layer material should be lightweight to minimize foreign-body sensation.

Given the soft and dynamic nature of human skin surface as substantiated by prior research,[20] multiple studies have explored diverse substrates and conductive materials for the fabrication of soft sensors. Various choices of on-body flexible electronic substrate are shown in Table 1.

Flexible electronics frequently employ plastic substrates, such as polyimide (PI), on conventional flex printed circuit boards (PCBs).[21,23] Nevertheless, these materials' intrinsic lack of stretchability and breathability confines their utility to planes and restricts their application on irregular body contours. Polydimethylsiloxane (PDMS), a kind of silicone rubber, has been widely used as insulating substrate for wearable electronics[24,25] and exhibits a degree of stretchability at 150%.[26] However, these materials encounter significant issues related to comfort: First, PI is stiff with a Young's modulus of up to 3.54 GPa, demonstrating poor skin compliance and unacceptable foreign-body sensation.[18] This kind of substrate contributes to a perceptible foreign-body sensation on the user's skin, particularly in joint areas. Second, the dense PDMS and PI substrates show poor breathability, hindering sweat evaporation during the on-skin scenario and potentially leading to skin irritation over prolonged periods of coverage.[27]

To meet the requirements for stretch sensing and wearable comfort, we adopted the poly(styrene-b-butadiene-b-styrene) (SBS) electrospun fiber mats developed in our previous research (WADE-skin),[27] which was validated as a substrate and cover for the on-body sensors.[22] This fiber mesh has been investigated for use while attached to the human body, maintaining good comfort originating from its textile-like breathability. Incorporating this into our prototype, the fiber mesh possesses a thickness of 0.2 mm, effectively mitigating the foreign-body sensation. To complement the poly(SBS) fiber, eutectic gallium-indium alloy (EGaIn) liquid metal was used for the conductive layer. EGaIn is a unique stretchable conductor that retains its liquid state at room temperature. It boasts several advantageous attributes including low viscosity, high conductivity, and high biocompatibility.[28]

For our application, leveraging these properties, liquid metal can be effectively coated or printed onto fiber-mat substrates and subsequently encapsulated with additional layers to create conductive, stretchable, and breathable sensor modules (see Figure 2D).

Sensor unit: Screen printing and characterization

The stretch sensor's physical performance is influenced by its pattern, with factors such as line geometry playing a crucial role in determining stretchability.[29,30] In our research, we have opted for a zigzag strain-gauge pattern as the base sensor unit with accurate unidirectional surface strain response to capture the most knee-surface deformation in a single direction.

Following the sensor unit's shape, we introduce an economical and rapid method for fabricating our standard stretch sensor, employing accessible materials and assets. The assembly process is demonstrated in Figure 2 and detailed in the methods section.

Post encapsulation, the gauge factor (GF) of this three-layer sensing unit is measured as 1.74 under the strain range of 0%–150%. A higher strain load may lead to disconnection of the conductive layer and influence the linearity of the sensor response. This sensor has good stretchability with a breaking strain of 900%. Based on actual operating conditions (covering the knee skin), this stain sensor will work under a 150% strain range. Each sensor unit shows resistance change linearity over 2,000 cycles of stretch in later bending and user studies. Each sensor unit measured dimensions of 10 cm in length, 4 cm in width, and 0.3 mm with a nominal resistance of 60 ± 5 Ω.

$$GF = \frac{\Delta R/R}{\Delta L/L}. \qquad \text{(Equation 1)}$$

Designed for human wearability, all the components (SBS mat and EGaIn liquid) of the sensor unit are non-toxic and well permeable with a porous structure. The thin, highly stretchable, permeable, and non-toxic nature of our sensor unit is exceptional for its long-term wearing comfort compared with commercial polyethylene terephthalate (PET) bending sensors.

Multi-channel sensor array

To transition the sensing technology to an integrated product, customizing sensor arrays for different anatomical regions of the human body provides versatile solutions that accommodate the dynamic nature of human physiology.[31] Considering the target area we planned to monitor, in prior clinical investigations, patients afflicted with arthritic joints frequently exhibited abnormal knee dynamics characterized by constrained bending angles.[32] Girth measurement in the clinic is usually undertaken in the context of both knees and thighs. Knees manifesting effusion display an associated knee-circumference swelling of approximately 2 cm.[33] Thigh circumference can also be used as a recovery test for the knee (measured 10 cm above the level of the knee patella) after knee-replacement surgery, where the joint is compromised and high muscle atrophy is present. In this setting, the thigh circumference decreases compared to the normal thigh circumference.[34]

A tailored sensor array has been developed to monitor joint swelling and associated muscle wasting simultaneously. As shown in Figure 2E, our knee-monitoring device incorporates three strain-gauge units: the joint-angle unit, the joint girth unit, and the thigh-girth unit. These sensors are arranged in a crossover pattern, forming a sensor array tailored to meet the demands of kinematic and swelling monitoring for users. The joint girth unit is strategically positioned in a circular pattern at

the level of the patella, enabling the recognition of knee swelling. The joint-angle unit traverses the patella vertically, facilitating knee flexion angle recognition. Lastly, the thigh-girth unit is situated 10 cm above the patella, serving to detect thigh muscle swelling or atrophy.

Data acquisition and system performance

The microcontroller unit (MCU) Seeed Studio XIAO Sense[35] is mounted on the sensor for analog data acquisition and Bluetooth transmission. The XIAO's size of 21 × 17.5 mm renders it highly suitable for integration into wearable devices. Furthermore, its ultra-low power consumption, registering at a mere 5 μA in deep-sleep mode, empowers it to efficiently manage lithium battery charging for extended durations.[35] The microcontroller is attached to the outside of a knee brace via a miniature battery that provides 3.3 V to the sensor. As Figure 2I shows, the I/Os are connected to the MCU analog input ports. The ADC resolution is 12 bits, so the smallest detectable voltage change is ΔV_o (0.805 mV). Three 220-Ω resistors are set as the voltage divider for each sensor, and the voltage under divider V can be measured using Equation 2. Furthermore, the resistance changes ΔR and the length changes ΔL were calculated based on the analog signals (A, A_0) from MCU, as shown by Equation 3. Under this circuit, the smallest 0.087-Ω resistance change ΔR_o can be detected as using Equation 4, and the smallest detectable strain ϵ_{min} is 0.0833% according to a GF value of 1.74.

$$V = \frac{3.3\text{V}\cdot 220\Omega}{R+220\Omega}, \qquad \text{(Equation 2)}$$

$$\Delta R = 220\Omega\left(\frac{1}{A}-\frac{1}{A_0}\right) = GF\cdot\frac{\Delta L}{L}\cdot R, \qquad \text{(Equation 3)}$$

$$\Delta R_o = \frac{\Delta V_o}{\frac{dV}{dR}} = \frac{0.805\text{mV}}{\frac{3.3\text{V}\cdot 220\Omega}{(60\Omega+220\Omega)^2}} \approx 0.087\ \Omega, \qquad \text{(Equation 4)}$$

$$\epsilon_{min} = \frac{\Delta R_o}{R\cdot GF} = \frac{0.087}{60\cdot 1.74} \approx 0.000833. \qquad \text{(Equation 5)}$$

The three-channel signal was collected at a frequency of 40 Hz to ensure adequate data on the surface deformation of the living knee. The sensor and MCU are finally integrated as the knee-monitoring device and placed on the patient's knee as shown in Figure 2J. In addition to fitting the knee-monitoring device directly to the skin, it is also possible to incorporate the product into commercially available knee pads or orthotics. For example, at the sacrifice of accuracy, a more adaptable knee brace can be worn with our knee-monitoring device inside, ideal for public use and in the hospital environment.

Personal information support

Our information support includes both real-time knee-state assessment and long-term cumulative knee-state analysis. The user interfaces are designed as shown in Figure 3. Personal information support can significantly help in health management and telemedicine, a health-monitoring system that combines sensing devices and features visualization apps or websites that can help users to conduct self-health assessments. To provide individuals with information support, we developed our digital platform combining an app and a website. The product is designed with the hypothetical goal of personal knee-health management in mind. To address the aforementioned need for both real-time monitoring and long-term assessment of arthritis status,[6] the device will offer two key features: real-time data display and cumulative knee-data statistics. The real-time data display is intended to serve as a potential alert for abnormalities, while the accumulated data statistics are aimed at providing a reference for assessing long-term knee health. The following sections detail the design and functionality of these support features.

Real-time data display

Our knee-monitoring app aims to offer real-time feedback while users are undertaking knee-state assessment or are under rehabilitation exercises. Real-time data display of certain body parts, such as muscles or joints, can help patients engage in rehabilitation exercises.[36] In our study, therefore, a mobile app was developed to display real-time knee-state data from our wearable knee-monitoring devices.

Cumulative data overview

Visualization of health-monitoring systems for everyday use also provides a user experience that includes an improved understanding of target indicators and increased acceptance of reminders to help patients with self-health management.[37] Visualized telemedicine systems can also help physicians rehabilitate patients or manage chronic conditions.[38]

Besides real-time monitoring on the mobile device, a web-based platform visualizes data from the database for long-term data analysis, which is also remotely accessible for researchers. The web shows the proportion of knee-swelling status over the whole testing period and also graphs the status distribution on the time (last hour, last day, last week). It helps doctors and patients understand the date the abnormality occurred and the degree of pre-existing knee swelling.

Machine-learning architecture and training

Joint-angle model development

To validate the feasibility and robustness of our designed wearable sensor, we adopt robotic arms to various movement angles and place our wearable sensor on the robotic arms to stretch and acquire various signals. As the robotic arms are already well-validated devices,[39] we adopt the movement angle of robotic arms as the labels and each sequence of the acquired data points as the input data. By removing the artifacts during the experiment (e.g., the beginning and ending moments of the robotic arms and some adjustments), the labeled data can be split into training and test data with the common ratio 8:2. The training data will be imported into ML models for training in order to detect the movement angle based on the input sensor signal. For the detection task, we select the random forest model that is widely adopted in pattern-recognition tasks[17] to show the best performance. Let us denote the random forest as RF[40] and suppose we have N trees in the forest. We can then denote the prediction of each tree as $h_i(x)$, where i ranges from 1 to N and x is the signal input data. The overall prediction $\hat{y}$ of the random forest for a given signal input x is typically the majority vote of the individual tree predictions. So, for a detection task, we can represent it mathematically as

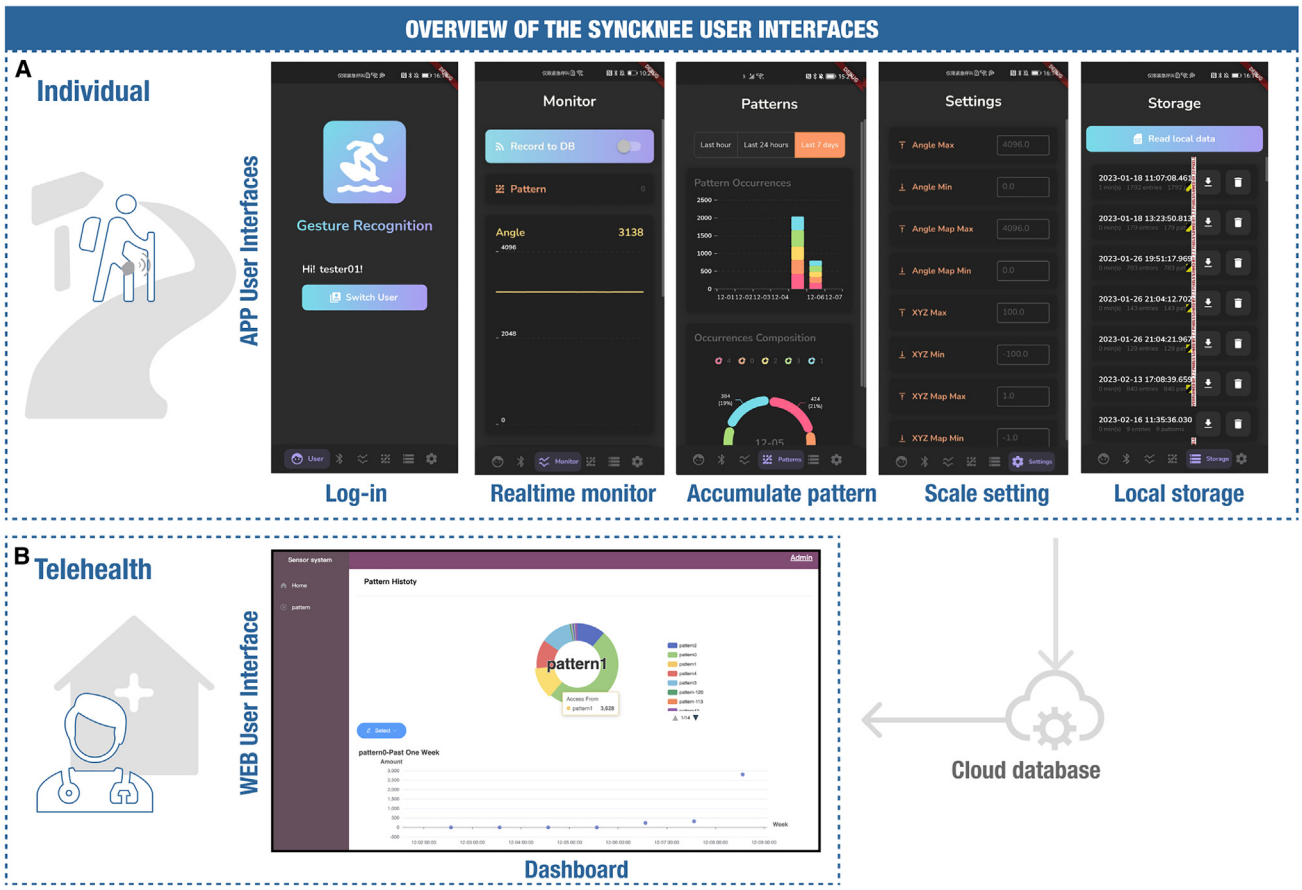

Figure 3. Overview of the SyncKnee user interfaces and system architecture

The SyncKnee system integrates individual (A) and telehealth (B) components. The app user interfaces include a log-in screen, a real-time monitor, pattern accumulation, settings configuration, and local storage. The web user interface for telehealth features a dashboard for pattern history visualization. Data are stored and managed in a cloud database, facilitating seamless information flow between the individual and telehealth interfaces.

$$\hat{y} = mode\{h_1(x), h_2(x), \ldots, h_N(x)\}.$$

Here, *mode* represents the mode function, which returns the most frequent value among the set of predictions.

Multi-channel data integration

To enhance the precision of predictions regarding human movement, participants were equipped with our specialized device and engaged in controlled walking experiments. To simulate a wide range of swelling conditions relevant to daily activities, we introduced a pump-swelling simulator within a pair of knee pads. The wearable sensor device was securely attached to the surface of the knee pads, allowing for the capture of dynamic signals during movements. Participants, while wearing the wearable device, were guided along purpose-built pedestrian pathways, maintaining a consistent step length throughout. Measurements were taken at two specific locations: around the knee at the level of the patella to assess joint swelling (referred to as "joint girth") and 10 cm above the patella border to evaluate muscle wasting (referred to as "thigh girth"). At the same time, based on the validated joint-angle random forest model, we can track the joint angles through human movements and save the data during user studies.

The signals collected through the wearable sensor are integrated with the joint-angle sequence as the input data, which is subsequently partitioned into distinct training and testing sets at a 9:1 ratio. Consistent with the training procedure outlined earlier, we adopt the random forest model to train a multi-channel knee-monitoring model based on the integrated data.

Data filtering

To reduce the effect of noise introduced by the sensor, a 6-order infinite impulse response (IIR) low-pass filter is designed. This is decided by empirical observations indicating that the relevant signal component predominantly occupies lower frequency ranges. Furthermore, the IIR filter offers low computational complexity and can achieve narrow pass bands with low orders, which are well suited to our requirements. The filter is configured with a normalized cutoff frequency of 0.2, and its frequency response is as follows:

$$H(z) = \frac{B(z)}{A(z)} = \frac{b(0)+b(1)z^{-1}+\cdots+b(6)z^{-6}}{a(0)+a(1)z^{-1}+\cdots+a(6)z^{-6}},$$

Table 2. IIR filter coefficients

$a(0)$	1	$b(0)$	9.1678×10^{-9}
$a(1)$	−5.6359	$b(1)$	5.5007×10^{-8}
$a(2)$	13.2451	$b(2)$	1.3752×10^{-7}
$a(3)$	−16.6142	$b(3)$	1.8336×10^{-7}
$a(4)$	11.7312	$b(4)$	1.3752×10^{-7}
$a(5)$	−4.4210	$b(5)$	5.5007×10^{-8}
$a(6)$	0.6947	$b(6)$	9.1678×10^{-9}

where the filter coefficients $a(0)$, …, $a(6)$ and $b(0)$, …, $b(6)$ are determined using the Butterworth method and are presented in Table 2. The frequency response of the designed filter is shown in Figure S1A.

Voltage output vs. skin deformation

Two experiments were conducted to test SyncKnee's output toward sense knee angle and girth change. Obtaining insights from previous studies, machine-assisted testing can ensure the accuracy of the featured data and the consistency of multiple measurements, e.g., the firmness test of wearable products.[41] Thus, in terms of the apparatus, we customized two devices to replicate knee-bending and -swelling features. The experimental apparatus and setup are shown in Figures 4A and 4B.

Robotic-arm-based bending test

For the evaluation of the joint-angle sensor, we customized a knee-bending device that adopted a reliable robotic arm to replicate bending of the human knee.

Air pump-based swelling test

As there is limited study on wearable solutions for swelling measurement and consequent evaluation approach, we built an air-pump-based swelling device to simulate the girth change under knee swelling. This test evaluates SyncKnee's response function to knee and thigh swelling under the noise from walking.

The detailed design and setup of the two tests can be found in the methods section.

Bending and swelling fit functions

According to results in Figure 4, our SyncKnee device responds effectively to changes brought about by bending and swelling. In our robotic-arm-based bending test, we observed a clear linear correlation between the change value (y_j) of the knee-monitoring device and the bending angle (x_j) at which the knee simulator was bent (Figure 4C). This correlation was established based on a generated linear fit function: $y_j = -2.11x_j + 380.08$. To clarify, the "change value" of the knee-monitoring device represents the disparity between its output at the target angle of the simulator and its output in its initial non-bending state (baseline), and this is a unitless quantity. This finding supports the utility of our knee-monitoring device's joint-angle sensor as an effective knee-flexion-angle detector. Furthermore, a durability test was conducted on the knee-monitoring device by undergoing 13 cycles of bending, each consisting of 50 repetitions (a total of 650 times for each test). Our sensor exhibited remarkable stability and robustness throughout these multiple bending conditions.

In the result of the air-pump-based swelling test, we observe that the value of the joint girth sensor correlates with knee swelling measured in advance, and the value of the thigh-girth sensor correlates with pre-assessed thigh circumference (the position 10 cm up from the knee patella). Considering an increase in knee swelling (Figure 4D), the output change of the joint girth sensor shows a quadratic change based on the generated fit function $y_J = -0.07x_J^2 + 51.53x_J - 6454.61$. Similarly, the thigh-girth sensor also shows a quadratic change (Figure 4E): $y_T = -0.05x_T^2 + 39.318x_T - 5674.08$ with thigh muscle waste (manifested as a decrease in thigh girth of the simulator). To summarize, these findings indicate that both girth sensor parts (joint and thigh) of the knee-monitoring device can stabilize the girth changes brought about by edema or atrophy in the corresponding parts. Generally, the fitted equations provide a valuable tool for assessing the extent of knee and thigh swelling in patients when compared to knee-circumference and leg-circumference measurements in a healthy state.

Knee-pattern recognition

Brief apparatus and procedures

After confirming SyncKnee's responsiveness to both joint angle and girth measurements, the system's feasibility in real-world user scenarios was further validated by integrating multi-channel signals to discern various knee-joint states. In contrast to solely relying on a single-channel goniometer to differentiate knee gait, our system incorporates variations in joint and thigh circumference to identify multiple knee states during daily activities, encompassing "stand," "sit," "knee raised," "squat," and "lunge." Despite similar knee angles, distinct expansions in knee and thigh muscles were observed during sit, knee raised, squat, and lunge actions. Manual knee-circumference measurements revealed marginal differences in knee girth across these five behaviors, averaging a 1.2165% change rate compared to the "stand" action, as depicted in Figure 5.

Recognition performance

Data from 15 individuals were first collected and processed using our ML model. 2,700 segmented action samples (80 data points per sample) were collected and split into training and testing sets using a standard 8:2 ratio. By comparison, we tested three models to classify the target behavior of 15 users. The IIR low-pass filter was then deployed to reduce the noise of raw data. Figure S1C shows the comparison between raw data captured by the sensor and filtered data by designed IIR filter of the "lunge" example of one subject. It is evident that the filter is capable of attenuating noise and smoothing the data.

The classification results are listed in Table 3. Notably, our random forest model demonstrated outstanding performance, achieving a high accuracy rate of 84.33% with raw data. For comparison experiments, we further included the data sequences by importing the filtered dataset and summarized all experimental results accordingly. We observed significant enhancements in classification accuracy with our designed IIR filter, achieving improvements of 0.43%, 16.71%, and 13.34% across three models. In the end, our SyncKnee integrated with the random forest algorithm achieves an outstanding classification accuracy of 98.48%. Among various knee behaviors, "stand," "sit," "lunge," and "knee raise" are identified with

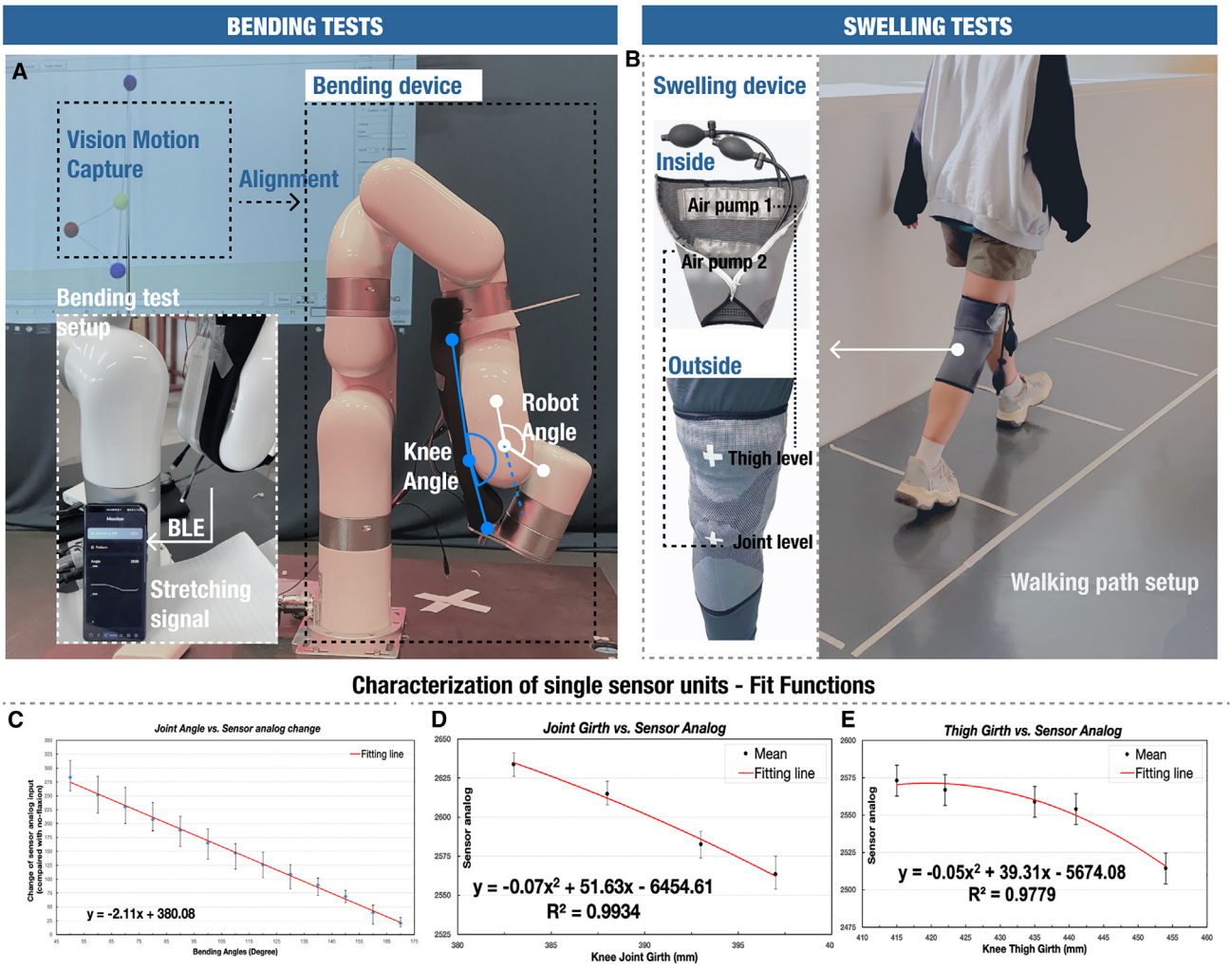

Figure 4. In-lab experiment

(A and B) 1: experimental setup for in-lab bending and swelling tests. (A) The bending test setup includes a vision motion-capture system for angle mapping and a bending device to simulate knee movement. The inset shows the stretching signal monitored via BLE. (B) Swelling test. The left panel shows the swelling device, including the inside view with air pumps 1 and 2, and the outside view indicating placement at the thigh and joint levels. The right panel illustrates the experimental setup used during the tests.

(C–E) 2: sensor response to three target features: (C) angle vs. sensor analog, (D) joint girth vs. sensor analog, and (E) thigh girth vs. sensor analog. Data represent mean ± SD.

greater ease (with an accuracy rate of 100%) compared to "squat" (with an accuracy rate of 94.12%).

These experiments, involving various exercise-induced knee changes, validated the proficiency of our multi-channel SyncKnee system in detecting comprehensive knee actions. The random forest-enabled SyncKnee model efficiently analyzes users' knee movements, contributing to its feasibility in discerning diverse knee states.

DISCUSSION

In this paper, we designed the SyncKnee system for daily knee monitoring. SyncKnee provides individuals with an effective approach to tracking their joint and muscle movement. Compared to previous studies, SyncKnee excels in more comprehensive knee assessment as well as high accuracy in knee-motion recognition and personal information support.

Key takeaways

Monitoring angle plus swelling

In this study, we aimed to assess multiple parameters of human knees for rendering a comprehensive knee status. Previous works are limited in assessing knee flexion through a goniometer. On the other hand, girth changes are commonly found in KOA patients,[3] but the girth measurement is merely accessible to individuals. In our method, therefore, knee-girth measurement was considered to argue for kinesthetic flexion. According to clinical guidance, we also provide separate channels on both

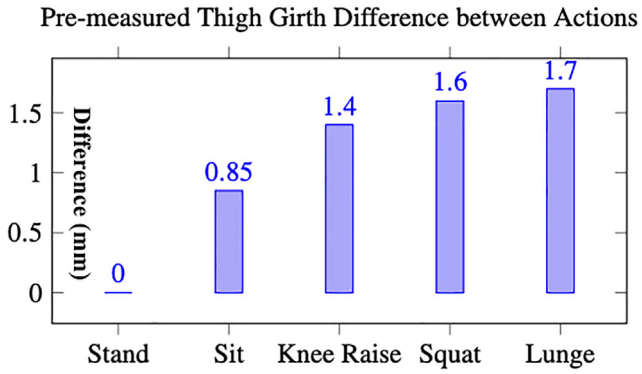

Figure 5. Manually measured thigh-girth difference between actions
The average change rate based on the "stand" action compared to the other four actions is approximately 1.2165%.

the knee-joint level and the thigh level to provide higher monitoring resolution. The sensor channel for the joint level responds directly to knee swelling under this joint, and the channel for the girth level reacts to the inflation on the target thigh muscle caused by swelling or weakness. Both channels show stable quadratic changes during the girth changes, demonstrating the ability of SyncKnee on knee-girth measurement. Along with the joint angle, SyncKnee can monitor three knee parameters simultaneously and pack them with time stamps. Our multi-channel solution excels in recognizing knee-joint behavior (even the behavior with similar flexion angles but differing in muscle conditions) and achieves a high detection performance. Based on our study, combining kinesthetic joint angles and the physiological parameters of muscle could give a more comprehensive joint assessment and help with detailed motion tracking.

Soft solution with advanced materials

Our soft sensor leverages the poly(SBS) mesh's stretchability, thinness, and breathability to maintain good comfort during daily monitoring. The material combination of poly(SBS) mesh and EGaIn liquid metal presents great potential in soft electronics.[22,27] Our study proves the concept of applying this state-of-the-art technique to human knees for skin-deformation measurements. Compared to commercial stretch sensors, SyncKnee enables on-body detection and is easier to attach to the skin without obvious foreign-body sensations. In addition, the thinness of SyncKnee's material allows a multi-layer structure to extend the functionality in one sensing area. With our sensor pattern design in different layers, SyncKnee can assess stretching on three different dimensions within a single pad, reducing the complexity of hardware for personal use.

In addition, our study provides detailed guidance for producing SyncKnee sensors. In this study, we adopted the screen-printing technique to transfer the liquid metal to our substrate. Screen printing is widely used in printing colorful ink onto our clothes and is also an accessible approach for many designers and design institutes. Our PET stencil with designed pattern and thickness ensures standard resistance of the fabricated sensor. This easy-to-fabricate approach moves from designing the pattern in CAD to cutting the PET stencil with a pattern before screen printing the liquid metal on the substrate. Our guidance can also help designers to customize and iterate their soft SyncKnee quickly.

Unified system with machine learning

This study targets personal knee-monitoring scenarios, and in this case an all-in-one system will be ideal for individuals. Apart from the sensor design, SyncKnee gives a united system incorporating ML models and information support. Previous work[17] evaluated various supervised ML algorithms on the gait feature classification. In our study, we also tested four ML models on our knee-monitoring system, in which random forest had the best classification accuracy of 98.48%. The random forest model in this study pre-trained with users' target knee actions translates the skin deformation on three channels into an easy-to-understand knee state. Our random forest model holds high classification accuracy with serious movements in one angle, i.e., lunges, knee raises, and squats. Therefore, the SyncKnee employing ML has the ability to perform precise knee-motion recognition and knee-state monitoring. Moreover, the personal information support covers the needs of real-time monitoring and the accumulated knee-status analysis, offering various applications in the future such as real-time abnormal notification and long-term rehabilitation validation.

Limitations of the study

This study is limited by participants and experimental time. Considering the scope of this study as a proof of concept and the recruitment difficulty in reaching out to KOA patients, we only conducted our experiments with healthy participants. Although our system performs well in recognizing different swellings caused by different exercises, considering the optimized system for precise classification of arthritis-related swelling, it will be helpful to have KOA patients involved in the future. In addition, in our pre-training, we collected a dataset of the user's short-term movements, whereby the model only classifies an instant pattern (sampling 20 times per second). The model lacks long-term clinical data from patients to enable training to obtain the correlation between a series of patterns and a certain arthritis symptom. To extend the ability of disease detection, the study needs more data from healthy people and knee patients to differentiate between short-term and long-term knee characteristics. Also in the user study, as the device was worn as an inner layer of a knee brace, there may be differences in the direct on-body application of the SyncKnee, and more experiments regarding the on-body situation need to be conducted to provide a more comprehensive ML model.

Potential applications and future work

Based on current knee-monitoring experiments by SyncKnee, we further showcase the potential applications of our system in KOA prevention and rehabilitation.

Real-time swelling alerts for outdoor activities

Compared with other wearable sensors, SyncKnee is comfortable to wear and more lightweight for outdoor activities. Besides, as shown in the app interface (Figure 3), SyncKnee provides real-time plotting graphs for knee-bending, knee-girth, and thigh-girth changes. At the top side of the user interface, we also provide a blank for knee patterns. For example, hikers can obtain the swelling patterns under current knee behavior, associating the

Table 3. Accuracy of various models for predicting knee-joint behavior

	Accuracy											
	Raw data						Filtered data					
Model	All	Stand	Sit	KR	Squat	Lunge	All	Stand	Sit	KR	Squat	Lunge
DT	0.8354	0.8118	0.8750	0.8243	0.8063	0.8554	0.8939	1	1	0.7059	1	0.9167
RF	0.8433	0.8325	0.8825	0.8145	0.83	0.8539	0.9848	1	1	1	0.9412	1
KNN	0.8421	0.8159	0.8736	0.8246	0.8254	0.8631	0.9545	1	1	0.8824	1	0.9167

The results were based on the filtered data from 15 participants. DT, decision tree; RT, random forest; KNN, nearest neighbors; KR, knee-raise activity.

swelling pattern with hiking behaviors, such as the knee-swelling pattern during continuous climbing or quick heavy landing. Users can track their knee-swelling status and notice abnormalities if there is still a high swelling pattern while relaxing or walking. This application can help with prevention of knee problems by acting as the pre-notice to avoid overused knee joints. The physical notification of SyncKnee could be further designed in the future to free users' eyes from their mobile phones.

Remote rehabilitation validation

A long-term assessment of the patient's knee state is crucial for evaluating the rehabilitation progress. SyncKnee's information system provides an accumulated patterns graph with a customized time range and can map the proportion of various knee patterns. Our website also allows remote access. Thus, SyncKnee enables telehealth to analyze the knee-state change over a timeline and the overview of a significant knee state, with the ultimate aim of validating individual rehabilitation progress.

METHODS

SyncKnee fabrication

(Step 1) The screen-printing process begins with the production of a stencil, wherein the conductive layer's pattern is meticulously designed. (Step 2) Subsequently, the PET sheet is cut with the designated pattern (if a laser cutter is unavailable, the pattern may be printed on the PET sheet and cut manually). (Step 3) This PET stencil is then positioned onto the targeted area of the fiber mat, followed by the uniform application of EGaIn liquid metal coating using a roller. The roller is systematically maneuvered over the stencil until the coating is fully transferred, allowing for the successful printing of the conductive layer onto the substrate. (Step 4) To increase the conductive area in the connection area, a 6.35-mm-wide double-sided copper conductive tape is employed to affix to both ends of the sensor for easy and robust wiring. (Step 5) After connecting the wires, the top layer is glued on to complete the quick encapsulation of a sensor unit. Note that the fabrication process of the poly(SBS) mesh layer is not the focus of this paper, for which readers are referred to the previous work on WADE-skin.[27]

Robotic-arm-based bending test

For the evaluation of the joint-angle sensor, we customized a knee-bending device that adopted a reliable robotic arm to replicate bending of the human knee. Within our study, the robotic arm is the Ufactory XArm 7,[42] a 7-joint robotic arm, which can rotate each joint to a certain angle precisely and also call back the motion angle. We used the sixth axis of the robotic arm to simulate the knee joint, and the joint-angle sensor was affixed to the gear using two stands and nylon ties, as illustrated in the accompanying Figure 4A. Considering errors due to fixtures, we also refer to the camera to compare the printed angle of the robotic arm with the actual bending angle of the knee-monitoring device assembled on its surface. A 7-cameras Eagle Digital System from Motion Analysis (USA), which is widely used in the field of motion-capture and joint-motion simulation,[43] was used as a pre-test to map the robotic arm's joint angle with the real bending angle of our sensor. The pre-test result shows that the printed angle from our robotic-arm-based bending device can be reliably mapped to the sensor's bending angle with a systematic error of only 0.66% with respect to camera motion tracking.

After the pre-test, knee-bending angle validation of our knee-monitor device based on this simulator was conducted. In the experiment, the sixth joint of the robotic arm was operated to move from the starting point (knee upright state, 180°) to the target bending point (50°–170°, the interval is 10°) and conducted 50 times for each target bending point. The knee-monitoring device's data were collected in the form of joint angle analog value time via Bluetooth with frequency 20 Hz and stored on the phone and cloud database.

Air-pump-based swelling test

This test evaluates SyncKnee's response function to knee and thigh swelling under the noise from walking. Polyurethane (PU) air pumps capable of achieving a uniform variation of 30 mm thickness were designed to be able to fit the human body as a swelling simulation. In addition to the static swelling simulation, with reference to the experimental setup regarding gait analysis,[44] this swelling simulation experiment was also performed while subjects were walking as instructed. We established a controlled pathway for our participants, limiting their number of steps (precisely 12 steps) and their stride length (65 cm) to validate the girth measurement. The experimental setup is shown in Figure 4B. Varying degrees of swelling in both the thigh and knee joints were assessed, from 42 cm to 45 cm circumference for the thigh and from 38.3 cm to 40 cm for the knee, respectively. These measurements represented different levels of swelling.

User study: Knee-pattern recognition

We recruited 15 participants on campus, all of whom are students. The cohort comprises five males and ten females whose ages range from 23 to 28 years (mean = 25.4, SD = 1.86), with diverse

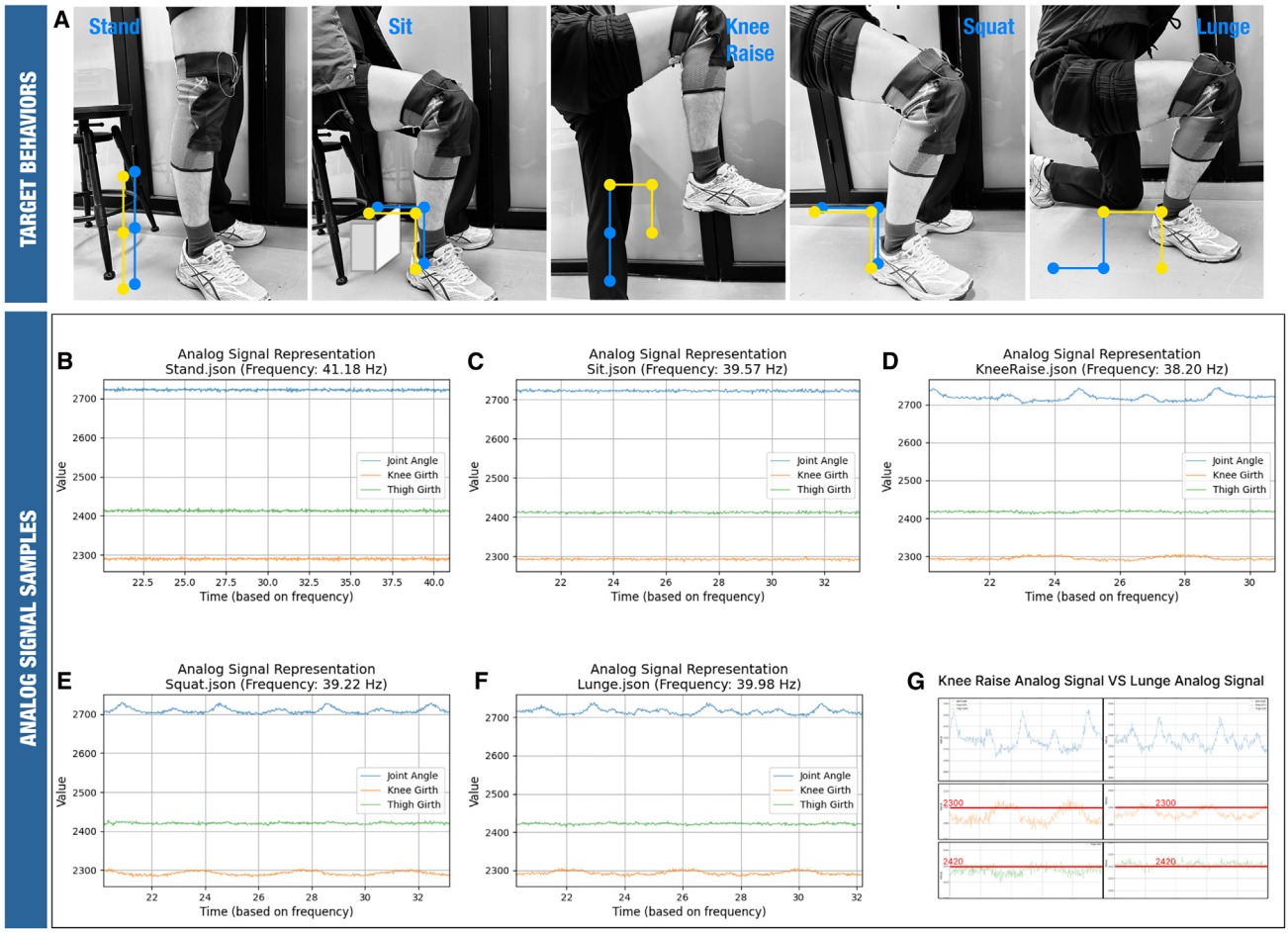

Figure 6. User study

(A) Target behaviors: stand, sit, knee raises, squats, and lunges.

(B–G) Analog signal samples for various movements. Analog signal samples were captured during (B) standing, (C) sitting, (D) knee raise, (E) squat, (F) lunges, and (G) comparison of knee-raise and lunge movements.

n = 15.

heights ranging from 152 cm to 179 cm (mean = 164.4, SD = 8.69). Participants reported having no previous KOA or experiencing any discomfort of the knees. All the exercises were conducted on participants' right knees, and our SyncKnee was set up correctly with the help of researchers. In this user study, participants engaged in five distinct procedures, as illustrated in Figure 6A. Each sequence involved executing the specified knee exercise ten times, guided by a 2-s metronome. The participants transitioned from one standing position to another standing posture, with each targeted knee state maintained for 1 s, ensuring the entire movement's completion within a controlled 2-s time frame. For exercises involving knee bending (sit, knee raise, squat, and lunge), a chair set at a fixed height was utilized to maintain the participants' knee-joint angle at 90°. All of the data, formatted as (time stamp, joint-angle signal, knee-girth signal, thigh-girth signal) at a sampling frequency of 40 Hz, were transmitted to the mobile app via Bluetooth. Figures 6B–6G show the signal samples for the five actions, showcasing distinct patterns across all three channels, particularly the different patterns in the thigh-girth and knee-girth signals.

RESOURCE AVAILABILITY

Lead contact

Requests for further information and resources should be directed to and will be fulfilled by the lead contact, Stephen Jia Wang (stephen.j.wang@polyu.edu.hk).

Materials availability

All materials generated in this study are available from the lead contact with a completed materials transfer agreement.

Data and code availability

- All data reported in this paper will be shared by the lead contact upon request.
- All original code has been deposited at the SyncKnee repository and is publicly available at https://github.com/leonardofang/Syncknee as of the date of publication.

- Any additional information required to reanalyze the data reported in this paper is available from the lead contact upon request.

ACKNOWLEDGMENTS

This research was partially funded by AiDLab (project code: RP2-4) under the InnoHK Research Clusters, Hong Kong Special Administrative Region Government; the HK PolyU's Strategic Importance Project (P0036851); the HK PolyU's Research Centre of Future (Caring) Mobility (P0042701); and the Projects of HK PolyU's Research Institute for IWEAR (P0039255). We also extend our heartfelt thanks to all the participants who were involved in this study.

AUTHOR CONTRIBUTIONS

Conceptualization, S.J.W., Z.M., L.F., and C.F.; methodology, Z.M., L.F., and C.F.; investigation, Z.M., L.F., C.F., and F.C.; writing – original draft, M.Z and L.F.; writing – review & editing, C.F., F.C., and S.J.W.; model training, L.F.; data filtering, B.C.; material & fabrication, F.C., Z.M., and S.P.X.; supervision, S.J.W. and Z.Z.

DECLARATION OF INTERESTS

The authors declare no competing interests.

SUPPLEMENTAL INFORMATION

Supplemental information can be found online at https://doi.org/10.1016/j.xcrp.2025.102438.

Received: June 24, 2024
Revised: November 26, 2024
Accepted: January 17, 2025
Published: February 20, 2025

REFERENCES

1. WHO. Osteoarthritis (2023). https://www.who.int/news-room/fact-sheets/detail/osteoarthritis.
2. He, Z., Liu, T., and Yi, J. (2019). A wearable sensing and training system: Towards gait rehabilitation for elderly patients with knee osteoarthritis. IEEE Sens. J. *19*, 5936–5945. https://doi.org/10.1109/JSEN.2019.2908417.
3. Inan, O.T., Whittingslow, D.C., Teague, C.N., Hersek, S., Pouyan, M.B., Millard-Stafford, M., Kogler, G.F., and Sawka, M.N. (2018). Wearable knee health system employing novel physiological biomarkers. J. Appl. Physiol. *124*, 537–547. https://doi.org/10.1152/japplphysiol.00366.2017.
4. Chuang, W.-C., and Chen, W.-L. (2019). Real-time monitoring for knee extensor muscle training with flexible sensors. J. Microelectromech. Syst. *28*, 1005–1012. https://doi.org/10.1109/JMEMS.2019.2941939.
5. Monsalve, J.T., Arnold, D., Yi, W.-J., and Saniie, J. (2019). Design flow of wearable internet of things (IoT) smart workout tracking system. In 2019 IEEE International Conference on Electro Information Technology (EIT) (IEEE), pp. 271–274. https://doi.org/10.1109/EIT.2019.8833917.
6. Karatsidis, A., Richards, R.E., Konrath, J.M., van den Noort, J.C., Schepers, H.M., Bellusci, G., Harlaar, J., and Veltink, P.H. (2018). Validation of wearable visual feedback for retraining foot progression angle using inertial sensors and an augmented reality headset. J. NeuroEng. Rehabil. *15*, 78. https://doi.org/10.1186/s12984-018-0419-2.
7. Radiological Society of North America (RSNA) and American College of Radiology (ACR). (n.d.). Knee MRI RadiologyInfo.org for patients. https://www.radiologyinfo.org/en/info/kneemr.
8. Abebe, G., Cavallaro, A., and Parra, X. (2016). Robust multi-dimensional motion features for first-person vision activity recognition. Comput. Vis. Image Understand. *149*, 229–248, Special issue on Assistive Computer Vision and Robotics - "Assistive Solutions for Mobility, Communication and HMI. https://doi.org/10.1016/j.cviu.2015.10.015. https://www.sciencedirect.com/science/article/pii/S1077314215002350.
9. Stetter, B.J., Ringhof, S., Krafft, F.C., Sell, S., and Stein, T. (2019). Estimation of knee joint forces in sport movements using wearable sensors and machine learning. Sensors *19*, 3690. https://doi.org/10.3390/s19173690. https://www.mdpi.com/1424-8220/19/17/3690.
10. McManigal, M., Wilson, R., McManigal, P., Beran, B., Wellsandt, E., and Markvicka, E.J. (2022). Fully Untethered and Stretchable Wearable Electronic Bandage for Measuring Knee Motion. In Design of Medical Devices Conference of Frontiers in Biomedical Devices, *84815*, pp. V001T04A002. https://doi.org/10.1115/DMD2022-1026.
11. Faisal, A.I., Majumder, S., Scott, R., Mondal, T., Cowan, D., and Deen, M.J. (2021). A simple, low-cost multi-sensor-based smart wearable knee monitoring system. IEEE Sens. J. *21*, 8253–8266. https://doi.org/10.1109/JSEN.2020.3044784.
12. Musculoskeletalkey. Measurement in rehabilitation (2019). https://musculoskeletalkey.com/measurement-in-rehabilitation/.
13. Kirwan, J.R., Byron, M.A., Winfield, J., Altman, D.G., and Gumpel, J.M. (1979). Circumferential measurements in the assessment of synovitis of the knee. Rheumatology *18*, 78–84.
14. Perrin, M., and Guex, J.J. (2000). Edema and leg volume: methods of assessment. Angiology *51*, 9–12.
15. Stranden, E. (1982). Comparison between surface measurements and water displacement volumetry for the quantification of leg edema. J. Oslo City Hosp. *31*, 153–155.
16. Ge, G., Cai, Y., Dong, Q., Zhang, Y., Shao, J., Huang, W., and Dong, X. (2018). A flexible pressure sensor based on rgo/polyaniline wrapped sponge with tunable sensitivity for human motion detection. Nanoscale *10*, 10033–10040.
17. Faisal, A.I., Mondal, T., Cowan, D., and Deen, M.J. (2022). Characterization of knee and gait features from a wearable tele-health monitoring system. IEEE Sens. J. *22*, 4741–4753.
18. Tokuda, Y., Sahoo, D.R., Jones, M., Subramanian, S., and Withana, A.F. (2021). Crafting tangible and interactive electrical components with liquid metal circuits. In Proceedings of the Fifteenth International Conference on Tangible, Embedded, and Embodied Interaction. TEI '21 (Association for Computing Machinery), pp. 1–11. https://doi.org/10.1145/3430524.3440654.
19. Lin, Y.-A., schraefel, m. c., Chiang, W.-H., and Loh, K.J. (2021). Wearable nanocomposite kinesiology tape for distributed muscle engagement monitoring. MRS Advances *6*, 6–13. https://doi.org/10.1557/s43580-021-00005-4.
20. Lim, C., Hong, Y.J., Jung, J., Shin, Y., Sunwoo, S.-H., Baik, S., Park, O.K., Choi, S.H., Hyeon, T., Kim, J.H., et al. (2021). Tissue-like skin-device interface for wearable bioelectronics by using ultrasoft, mass-permeable, and low-impedance hydrogels. Sci. Adv. *7*, eabd3716. https://doi.org/10.1126/sciadv.abd3716.
21. Wang, Y., Xu, C., Yu, X., Zhang, H., and Han, M. (2022). Multilayer flexible electronics: Manufacturing approaches and applications. Materials Today Physics *23*, 100647. https://doi.org/10.1016/j.mtphys.2022.100647. https://www.sciencedirect.com/science/article/pii/S2542529322000451.
22. Ma, Z., Huang, Q., Xu, Q., Zhuang, Q., Zhao, X., Yang, Y., Qiu, H., Yang, Z., Wang, C., Chai, Y., and Zheng, Z. (2021). Permeable superelastic liquid-metal fibre mat enables biocompatible and monolithic stretchable electronics. Nat. Mater. *20*, 859–868. https://doi.org/10.1038/s41563-020-00902-3.
23. PCBONLINE. Website title (2022). https://www.pcbonline.com/blog/flexible-pcb-manufacturing-process.html sep 26, 2023.
24. Glauser, O., Panozzo, D., Hilliges, O., and Sorkine-Hornung, O. (2019). Deformation capture via soft and stretchable sensor arrays. ACM Trans. Graph. *38*, 1–16. https://doi.org/10.1145/3311972.
25. Yuan, X., Zou, J., Sun, L., Liu, H., and Jin, G. (2019). Soft tactile sensor and curvature sensor for caterpillar-like soft robot's adaptive motion. In

Proceedings of the 2019 International Conference on Robotics, Intelligent Control and Artificial Intelligence. RICAI '19 (Association for Computing Machinery), pp. 690–695. https://doi.org/10.1145/3366194.3366318.

26. Fan, Y., Pietroni, N., and Ferguson, S. (2023). A neural network-based low-cost soft sensor for touch recognition and deformation capture. In Proceedings of the 2023 ACM Designing Interactive Systems Conference. DIS '23 (Association for Computing Machinery), pp. 889–903. https://doi.org/10.1145/3563657.3595963.
27. Chen, F., Zhuang, Q., Ding, Y., Zhang, C., Song, X., Chen, Z., Zhang, Y., Mei, Q., Zhao, X., Huang, Q., and Zheng, Z. (2023). Wet-adaptive electronic skin. Adv. Mater. *35*, 2305630.
28. Dickey, M.D., Chiechi, R.C., Larsen, R.J., Weiss, E.A., Weitz, D.A., and Whitesides, G.M. (2008). Eutectic gallium-indium (egain): A liquid metal alloy for the formation of stable structures in microchannels at room temperature. Adv. Funct. Mater. *18*, 1097–1104. https://doi.org/10.1002/adfm.200701216.
29. Abu-Khalaf, J., Saraireh, R., Eisa, S., and Al-Halhouli, A. (2018). Experimental characterization of inkjet-printed stretchable circuits for wearable sensor applications. Sensors *18*, 3476. https://doi.org/10.3390/s18103476. https://www.mdpi.com/1424-8220/18/10/3476.
30. Cui, Z., Poblete, F.R., Cheng, G., Yao, S., Jiang, X., and Zhu, Y. (2015). Design and operation of silver nanowire based flexible and stretchable touch sensors. J. Mater. Res. *30*, 79–85. https://doi.org/10.1557/jmr.2014.347.
31. Markvicka, E., Wang, G., Lee, Y.-C., Laput, G., Majidi, C., and Yao, L. (2019). Electrodermis: Fully untethered, stretchable, and highly-customizable electronic bandages. In Proceedings of the 2019 CHI Conference on Human Factors in Computing Systems (Association for Computing Machinery), pp. 1–10. https://doi.org/10.1145/3290605.3300862.
32. Stiffler, M.R., Pennuto, A.P., Smith, M.D., Olson, M.E., and Bell, D.R. (2015). Range of motion, postural alignment, and less score differences of those with and without excessive medial knee displacement. Clin. J. Sport Med. *25*, 61–66. https://journals.lww.com/cjsportsmed/fulltext/2015/01000/range_of_motion,_postural_alignment,_and_less.9.aspx.
33. Suchy, J.P., Glasoe, W.M., and Koehler, L.A. (2023). A tissue dielectric constant evaluation of knee edema: A retrospective intra-rater reliability and association study of repeated measures. Cureus *15*, e42089.
34. Akima, H., and Furukawa, T. (2005). Atrophy of thigh muscles after meniscal lesions and arthroscopic partial menisectomy. Knee Surg. Sports Traumatol. Arthrosc. *13*, 632–637. https://doi.org/10.1007/s00167-004-0602-9.
35. Studio, S. Seeed Studio XIAO nrf52840 Sense - tinyml/tensorflow lite- imu/microphone - bluetooth5.0 (2022). https://www.seeedstudio.com/Seeed-XIAO-BLE-Sense-nRF52840-p-5253.html.
36. Zhu, J., Lei, Y., Shah, A., Schein, G., Ghaednia, H., Schwab, J., Harteveld, C., and Mueller, S.M. (2022). Improving unsupervised physical rehabilitation by monitoring and visualizing muscle engagement. In Proceedings of the 35th Annual ACM Symposium on User Interface Software and Technology (Association for Computing Machinery), pp. 1–14. https://doi.org/10.1145/3526113.3545705.
37. Neef, C., Linden, K., and Richert, A. (2023). Exploring the influencing factors on user experience in robot-assisted health monitoring systems combining subjective and objective health data. Appl. Sci. *13*, 3537. https://doi.org/10.3390/app13063537. https://www.mdpi.com/2076-3417/13/6/3537.
38. Vlasakova, M., Muzik, J., Holubová, A., Fiala, D., Arsand, E., Urbanová, J., Janíčková Žďárská, D., Brabec, M., and Brož, J. (2023). A telemedicine system intervention for patients with type 1 diabetes: Pilot feasibility crossover intervention study. JMIR Form. Res. *7*, e35064. https://doi.org/10.2196/35064.
39. Shahria, M.T., Arvind, A., Iqbal, I., Saad, M., Ghommam, J., and Rahman, M.H. (2023). Vision-based localization and tracking of objects through robotic manipulation. In 2023 IEEE 14th International Conference on Power Electronics and Drive Systems (PEDS) (IEEE), pp. 1–6.
40. Breiman, L. (2001). Random forests. Mach. Learn. *45*, 5–32.
41. Yang, Y., Ren, L., Chen, C., Wang, X., Fan, Y., Shao, Y., Zhu, K., Li, J., Wang, Q., Sun, L., et al. (2023). E-orthosis: Augmenting off-the-shelf orthoses with electronics. In Proceedings of the 2023 CHI Conference on Human Factors in Computing Systems. CHI '23 (Association for Computing Machinery), pp. 1–15. https://doi.org/10.1145/3544548.3581471.
42. Ufactory. xarm collaborative robot (2023). https://www.ufactory.cc/xarm-collaborative-robot/.
43. Lo, W.-T., Yick, K.-L., Lau, N., Tse, L.-T., Ng, S.-P., and Yip, J. (2017). Effects of slipper features and properties on walking and sit-to-stand tasks of older women. J. Aging Phys. Act. *25*, 587–595. https://doi.org/10.1123/japa.2016-0298. https://journals.humankinetics.com/view/journals/japa/25/4/article-p587.xml.
44. Zhou, L., Tunca, C., Fischer, E., Brahms, C.M., Ersoy, C., Granacher, U., and Arnrich, B. (2020). Validation of an IMU gait analysis algorithm for gait monitoring in daily life situations. In 2020 42nd Annual International Conference of the IEEE Engineering in Medicine Biology Society (EMBC) (IEEE), pp. 4229–4232. https://doi.org/10.1109/EMBC44109.2020.9176827.